1-1-2013

Work hardening behaviors of a low carbon Nb-microalloyed Si-Mn quenching-partitioning steel with different cooling styles after partitioning

Jun Zhang
Northeastern University

Hua Ding
Northeastern University

Chao Wang
Northeastern University

Jingwei Zhao
University of Wollongong, jzhao@uow.edu.au

Ting Ding
Northeastern University

Work hardening behaviors of a low carbon Nb-microalloyed Si-Mn quenching-partitioning steel with different cooling styles after partitioning

Abstract

In this paper, the strain hardening behaviors of a low carbon Nb-microalloyed Si–Mn quenching–partitioning (Q–P) steel were investigated. The microstructures were analyzed by the scanning electron microscope (SEM) and transmission electron microscope (TEM). Mechanical tests were used to evaluate the room temperature tensile properties of the steel. The work hardening behaviors of the tested specimens were analyzed using the Hollomon approach. The results showed that a two-stage work hardening behavior was observed during deformation processes. In the first stage, for the quenched samples, martensite deforms plastically and the hardening exponent decreased. For the air-cooled samples, however, the carbide-free ferrite deforms preferentially, and then, the carbide-free ferrite and martensite co-deform. In the second stage, due to the effect of transformation induced plasticity of retained austenite, the hardening exponent decreased slowly and plateaus were observed in the plots of ni–εt until fracture. Variations of the work hardening behaviors were related to the martensite and the volume fraction of retained austenite in Q–P steels and the microstructural evolution during partitioning and following cooling process.

Keywords

styles, cooling, different, steel, partitioning, quenching, mn, si, microalloyed, low, behaviors, after, hardening, nb, work, carbon

Disciplines

Engineering | Science and Technology Studies

Publication Details

Zhang, J., Ding, H., Wang, C., Zhao, J. & Ding, T. (2013). Work hardening behaviors of a low carbon Nb-microalloyed Si-Mn quenching-partitioning steel with different cooling styles after partitioning. Materials Science and Engineering A: Structural Materials: Properties, Microstructure and Processing, 585 132-138.

Work hardening behaviors of a low carbon Nb-microalloyed Si-Mn quenching-partitioning steel with different cooling styles after partitioning

Jun Zhang [a], Hua Ding [a, *], Chao Wang [a], Jingwei Zhao [b], Ting Ding [a]

[a] School of Materials and Metallurgy, Northeastern University, Shenyang, 110819, P.R.China

[b] School of Mechanical, Materials and Mechatronic Engineering, University of Wollongong, NSW 2522, Australia

[*] Corresponding author: Hua Ding.

E-mail address: dingneu@163.com (Hua Ding)

Tel.: +86-024-83673081; Fax: +86-024-23906316.

Abstract

In this paper, the strain hardening behaviors of a low carbon Nb-microalloyed Si-Mn quenching-partitioning (Q-P) steel were investigated. The microstructures were analyzed by scanning electron microscope (SEM) and transmission electron microscope (TEM). Mechanical tests were used to evaluate the room temperature tensile properties of the steel. The work hardening behaviors of the tested specimens were analyzed using Hollomon approach. The results showed that a two-stage work hardening behavior was observed during deformation processes. In the first stage, for the quenched samples, martensite deforms plastically and the hardening exponent decreased. For the air-cooled samples, however, the carbide-free ferrite deforms preferentially, and then, the carbide-free ferrite and martensite co-deform. In the second stage, due to the effect of transformation induced plasticity of retained austenite, the hardening exponent decreased slowly and plateaus were observed in the plots of n_i-ε_t until fracture. Variations of the work hardening behaviors were related to the martensite and the volume fraction of retained austenite in Q-P steels and the microstructural evolution during partitioning and following cooling process.

Keywords: Q-P process; Mechanical properties; Microstructure; Work hardening; Air-cooling

1. Introduction

The past decades have witnessed the development of high strength low alloy steels, martensitic steels, and dual phase steels with yield strength higher than C-Mn steels. Advanced high-strength steels (AHSS) contain a ferrite-bainite matrix with a few contents of martensite and a certain amount of retained austenite. Due to their good combination of excellent strength and ductility, AHSS have been investigated extensively [1]. Quenching-partitioning (Q-P) and quenching-partitioning-tempering (Q-P-T) steels have been developed to provide excellent mechanical properties among AHSS, and several studies have been carried out on these steels to their high feasibility for industrial production [2-5]. Q-P process consists of a two-step heat-treatment. The desired martensite fraction is, at first, obtained by quenching steels from the fully austenite or intercritical field to the desired quenching temperature. In the second step, the quenched steels are held at the temperature same with or higher than the quenching temperature to enrich retained austenite (RA) with carbon from the carbon supersaturated martensite [6]. In Q-P steels, martensite plays a role in enhancing the strength, and RA appears to be effective in the increment of plasticity, due to the effect of delayed fracture during deformation process [7].

In the beginning of the study, the Q-P treatment had been mainly performed on the low carbon transformation-induced plasticity (TRIP) steels in order to attain potentially higher strength levels by replacing bainite with martensite. One important phase in the TRIP steels is metastable RA, which is obtained by carbon enrichment of austenite during intercritical annealing and bainitic transformation [8-10]. The formation process of RA in Q-P steels is similar to that in TRIP steels. The carbon diffusional kinetics and martensite-austenite interface migration dynamics during the microstructural evolution have been researched based on a postulated “constrained carbon equilibrium” (CCE) [11,12]. Research on the mechanical properties of low and medium carbon Q-P steels under different heat-treatment conditions has been very active during the past several years [2-5].

In order to obtain the two-phase (martensite and RA) microstructure, Q-P steels are usually quenched after partitioning either treated by salt bath or continuous annealing equipment. In view of industrial production, the continuous annealing equipment is more suitable for the production of Q-P steels. In view of the coiling process after continuous annealing in the practical production, the air-cooling style after partitioning offers an effective approach to simplify the heat treatment process and the production cost savings could be realized. Q-P steels can be easily coiled at partitioning temperature due to their lower strength relative to that of final products. However, the effects of air-cooling process after partitioning on the mechanical properties of Q-P steels have not been well documented. In particular, the work hardening behaviors of Q-P steels treated by different partitioning temperatures have been less investigated extensively.

The purpose of the present study was to simulate the coiling process of the low carbon Si-Mn steels in practical production by an air-cooling process after partitioning. The effects of cooling styles on the microstructures, mechanical properties and work hardening behaviors of a low-carbon Nb-microalloyed Si-Mn steel were systematically investigated. The effects of RA volume fraction on the work hardening exponents were also analyzed.

2. Experimental procedure

A low carbon Nb-microalloyed Si-Mn steel was used in this research. The chemical compositions of the steel are given in Table 1. In the studied steel, the elimination or suppression of the formation of cementite during the isothermal process is achieved by the addition of Si [13] and Al [14] and the low carbon content is applied to keep good weldability [15]. Manganese has an effect of decreasing the starting temperature of martensite transformation (M_s) and expanding the austenitic phase zone [16]. Besides above elements, microalloying elements, such as Nb, play an important role in improving strength without reducing ductility [17, 18]. The casting ingots were manufactured by a vacuum induction melting method. Ingots were homogenized at 1200 ℃ for 2h,

and then hot forged to slabs with width of 100 mm and thickness of 30 mm. These bars were heated to 1200 ℃, then held for 2h, and finally hot rolled to sheets with thickness of 3 mm after eight passes rolling with the start and finish temperatures of 1150 ℃ and 850 ℃, respectively. These sheets were air cooled to room temperature after rolling, and then cold rolled to strips with thickness of 1.2 mm by five passes rolling after pickling in 10 % hydrochloric acid.

Before Q-P treatment, dilatometer test was carried out to determine the austenitization starting (A_{c1}) and finishing (A_{c3}) temperatures in heating, as well as the M_s in cooling. The dilatometric curve of the steel is shown in Fig. 1. The A_{c1}, A_{c3} and M_s temperatures were determined as 720 ℃, 890 ℃ and 380 ℃, respectively. All the specimens were austenitized at 900 ℃ for 3 min, and then quenched to 260 ℃ in order to acquire the microstructure with the approximate volume fractions of martensite and RA. The quenched specimens were then directly transferred to a salt bath with different temperatures from 350 ℃to 450 ℃ for 120s. After being held at these temperatures for 120 s, some specimens were quenched in water - expressed as QPQ, and the others were air cooled to room temperature – expressed as QPA. The schedule for Q-P heat-treatment cycle is schematically shown in Fig. 2.

After heat treatment, rectangular tensile specimens (width 12.5 mm, thickness 1.2 mm, and gauge length 25 mm) were prepared along the rolling direction. Tensile tests were performed on a SANSCMT-5000 tensile machine at room temperature with the strain rate of 2×10^{-4} s^{-1}.

Microstructures were analyzed by scanning electron microscope (SEM) and a TECNAI-Q2-20 transmission electron microscope (TEM). The volume fraction of RA was measured via X-ray diffraction (XRD) with CuKα radiation operated at 40kV and 100mA. Samples were scanned from 40° to 120°, at a scanning rate of 2°/min. The volume fraction of RA (V_γ) was calculated by using the following equation [19, 20] :

$$V_\gamma = \frac{1.4I_\gamma}{I_\alpha + 1.4I_\gamma} \quad (1)$$

where I_γ and I_α are the integrated intensities of austenite and ferrite diffraction lines, repectively.

In the present work, the diffraction lines of $(200)_\alpha$, $(211)_\alpha$, $(200)_\gamma$, $(220)_\gamma$ and $(311)_\gamma$ were employed to determine the value of V_γ [20].

3. Results

3.1 Microstructures

The SEM microstructures of the Q-P treated samples are shown in Fig. 3. As shown in Fig. 3a through d, the QPA samples consist of irregular carbide-free ferrite (black), sometimes called "bainitic ferrite" [21], and martensite (light). For the QPQ samples, however, the microstructure is almost composed of full martensite (Fig. 3e through h). The SEM micrographs also indicate that all the martensite structures in the both sets of samples show a roughening trend with the increase of temperature. This microstructural characterization after Q-P treatment has also been reported elsewhere [22]. It should be mentioned that it is hard to distinguish the RA clearly in the SEM micrographs for the both sets of samples.

Fig.4 shows the TEM micrographs of RA in the undeformed samples partitioned at 390 ℃. It is clear that the flake-like RA is surrounded by lath martensite, which is transformed from the original austenite grains during quenching to 260 ℃. The observation of flake-like RA confirms that the transformation of martensite during the quenching process has an effect of mechanically stabilizing the adjacent flake-like austenite between lath martensites due to the three-dimensional hydrostatic pressure, which is one of the reasons to stabilize the RA at room temperature. The N-W relationship: [001]α // [011]γ, α // γ between the RA and lath martensite confirms that the habit plane exists during transformation from austenite to martensite. As shown in Fig. 4d through e, the α-γ interface observed in the QPA samples exhibits a bended shape. A higher partitioning temperature or longer partitioning time leads to stronger recovery of martensite, which makes the α-γ interface migrate significantly and finally become bended [23]. In the current study, the

air-cooling process with a relatively slow cooling rate is regarded as the continuation of partitioning, which prolongs the partitioning time and results in a bended α-γ interface. For the QPQ samples, however, the α-γ interface appears straighter than that in the QPA samples, as shown in Fig. 4a through b. It is thought that the relatively short partitioning time and the subsequent quenching process are responsible for this feature retained to room temperature.

3.2 Mechanical properties

The dependence of yield strength (YS), ultimate tensile strength (UTS), total elongation (TE), and product of strength and elongation (PSE) of the tested steel on partitioning temperature is shown in Fig.5. It can be seen that the YS, UTS and TE of the QPQ samples exhibit a decreasing tendency with increasing the partitioning temperature, and the maximum values of YS, UTS and TE are obtained as 1140 MPa, 1310 MPa and 12 %, respectively, at the partitioning temperature of 350 ℃. However, under air-cooling condition, the YS and UTS decrease gradually with temperature at first, then to a minimum value at 390 ℃, and finally they increase when the temperature is higher than 390 ℃, as shown in Fig. 5a. The TE and PSE of the QPA samples increase over the temperature range from 350 ℃ to 420 ℃, and then it decreases sharply when the temperature is higher than 420 ℃, as shown in Fig. 5b. It is worth noting that, the TE and PSE of QPA samples has a remarkable improvement in contrast to the TE and PSE of the QPQ samples, especially at the partitioning temperature of 420 ℃. This remarkable improvement of ductility is considered to be caused by the different final cooling styles, which has not been reported.

Fig. 6 shows the volume fraction of RA in the undeformed samples. It can be seen that the both sets of samples (QPA and QPQ) have significant difference in the volume fraction of RA at different partitioning temperatures. With the increase of partitioning temperature from 350 ℃ to 420 ℃, the volume fraction of RA in the QPQ samples changes slightly. When the partitioning temperature is increased to 450 ℃, the precipitation of cementite will occur, and carbon dilution in

austenite will be caused, finally the stabilization of the RA will be decreased. Therefore, the volume fraction of RA decreases at 450 ℃. However, in contrast to the QPQ samples, the volume fraction of RA has an significant increase for QPA samples. It can be due to the formation of carbide-free ferrite (Fig. 3) which results in the concentration of carbon in the untransformed austenite and further stabilizes this part of austenite. For the same reason with QPQ samples, the retained austenite in QPA samples decreases sharply when the partitioning temperature reaches 450 ℃.

3.3 Work-hardening behaviors

The work hardening behaviors were analyzed by using the following Hollomon equation: [24]

$$\sigma_t = K\varepsilon_t^{n_i} \tag{2}$$

where σ_t and ε_t are the true stress and true strain, respectively, K is the strength coefficient, and n_i is the instantaneous work hardening exponent.

The instantaneous work hardening exponent, n_i, can be deduced from the Eq. (2)

$$n_i = (\varepsilon_t/\sigma_t)(d\sigma_t/d\varepsilon_t) \tag{3}$$

where the n_i, σ_t and ε_t in Eq. (3) are the instantaneous work hardening exponent, the true stress and the true strain, respectively.

The plots of n_i-ε_t of the Q-P treated samples with different partitioning temperatures and different cooling methods after partitioning were illustrated in Fig. 7. For comparison, n_i-ε_t plots of a sample directly quenched from 900 ℃ to room temperature are also illustrated in Fig. 7. The martensite fraction of the sample directly quenched from 900 ℃ to room temperature is obtained to be 98 % by using the Koistinen-Marburger relationship [25]. In the current study, since the directly quenched sample has little RA, the TRIP effect can be also ignored. It is clear that all samples exhibit a two-stage deformation process except the directly quenched sample which only has one stage during the deformation. As shown in Fig.7, the n_i values of the first stage for all the samples decrease with increasing the partitioning temperature. In the second stage, the n_i values of

all the samples are almost unchanged and sustained through to the fracture, but the n_i values of the QPA samples exhibit a higher value than those of the QPQ samples at this stage.

The QPA samples at 390 ℃ have a higher strain than that at 350 ℃and 450 ℃. In addition, a more remarkable two-stage work hardening of the QPA samples is observed at 390 ℃ than that at 420 ℃. In order to further understand the two-stage work hardening behaviors of both the QPA and QPQ samples during the deformation, the volume fraction of RA of these two sets of samples (partitioned at 390 ℃) at different strain levels were measured by X-ray diffraction. The measured data presented in Fig. 8 indicates a variation of the volume fraction with engineering strain, revealing that the QPA samples have a higher initial volume fraction of RA than the QPQ ones. The RA volume fraction of both the QPA and QPQ samples exhibits a slightly decreasing rate in the early stage of strain (~0.06 for QPQ samples and ~0.08 for QPA ones). When the strain exceeds the critical value, a significant decrease of RA volume fraction is observed in Fig. 8 for these two sets of samples, which is attributed to the continuous martensitic transformation of RA and can be treated as the second stage of the work hardening.

4. Discussion

An interesting feature of the QPA samples is the presence of a certain amount of carbide-free ferrite (dark areas) in Fig.3a through d, which has not been reported in the previous researches on Q-P steels. In this research, all the samples, quenched from 900 ℃ to 260 ℃, form a certain amount of martensite and still 30 % (volume fraction) austenite is retained based on the Koistinen-Marburger relationship [25]. During the partitioning process, the martensite shows recovery characteristics (Fig. 3) and the RA is enriched by the diffused carbon. However the initial carbon content in the steel is insufficient to make all the 30 % RA stable at room temperature, which means some of the RA will transform to other phases. The work of Zaefferer et al. [26] on a low alloyed TRIP steel indicated that γ grains shrink and the volume fraction of carbide-free ferrite

increases with the increase of holding temperature and time. If the steel is held long enough in the bainite region, however, much of the metastable austenite will be replaced by carbide-free ferrite. In the present work, the partitioning temperature is in the temperature range of the bainitic transformation, and the metastable RA will transform to carbide-free ferrite when partitioned long enough at a temperature higher than M_s. Due to a much smaller cooling rate in air-cooling than in quenching, the air-cooling process can be considered as a continuation of partitioning, prolonging the partitioning time. Owing to the low solubility of carbon in carbide-free ferrite, carbon will diffuse to the untransformed austenite during the formation of carbide-free ferrite. This process increases the carbon content in the RA and improves the chemical stability of the RA. In addition, the volume expansion caused by the formation of carbide-free ferrite results in the increase of the three-dimensional hydrostatic pressure on the RA, which improves the mechanical stability of the RA as well [27]. Consequently, as shown in Fig. 6, the RA volume fraction in the final microstructure of the QPA samples is higher than that of the QPQ samples.

Fig. 7 shows both the QPQ and QPA samples exhibit a two-stage work hardening behavior. In the early strain stage, the n_i values of both the QPQ and QPA samples solely decreases from high initial value. The higher volume fraction of the hard phase, the higher work hardening exponent at the initial strain is expected [28, 29]. The higher initial n_i value of the QPQ samples than that of the QPA ones is attributed to the higher volume fraction of martensite in the QPQ samples. For both sets of samples, the strength of martensite decreases gradually with the increase of partitioning temperature, and correspondingly a gradually decrease in initial n_i is obtained. In order to prove this viewpoint, the n_i-ε_t plots of the sample, directly quenched from 900 ℃ to room temperature, was illustrated in Fig. 7. It has the highest initial n_i among all the samples.

Previous studies have shown that the instantaneous work hardening exponents of TRIP steels in the TRIP effect stage exhibit a large plateau before break [28]. In this stage, the transformation of RA relieves the local stress concentration caused by deformation, which delays the generation of

microcracks [30]. This delays the necking at the high strain and further enhances the elongation of the experimental steel. As a result of the higher volume fraction of RA in the QPA samples, the plateau of the QPA samples is larger than that of the QPQ ones, as shown in Fig. 7. That is, the QPA samples still have some of the RA available for transformation at a higher strain whereas the RA has been exhausted in the QPQ samples. Therefore, as shown in Fig. 5, the QPA samples have a relatively high elongation.

It is clear that the QPQ samples have a relatively lower n_i than the QPA ones at the end of the first stage, and the onset strain of the QPQ samples is also lower than that of the QPA ones. This may be due to the difference in microstructures between the QPQ and QPA samples. The QPQ samples consist of martensite and RA, and the martensite deforms plastically in the early strain stage. As martensite possesses high strength and low ductility, the local stress concentration occurs when the strain is small, and then, the RA will transform in order to relieve the local stress concentration. Therefore, the onset strain of the second stage is small. For the QPA samples, however, the carbide-free ferrite deforms preferentially in this stage due to its low strength and good ductility. As a result of work hardening, the strength of carbide-free ferrite increases. When the yield strength of martensite is reached, the martensite deforms plastically as a result of the load transfer. Therefore, the onset strain of the second stage of the QPA samples is higher than that of the QPQ ones. As shown in Fig. 7, at the end of the first stage, the n_i of the QPQ samples (about 0.1) are much smaller than that of the QPA ones (about 0.2), which proves that the QPA samples have a higher deformation ability.

It is worth noting that the volume fraction change of RA can be divided into two stages (Fig. 8), which is consistent with the two stages of work hardening (Fig. 7). When the strain is relatively low, there is no obvious change in the volume fraction of RA, while the RA decreases remarkably when the strain reaches a certain level, indicating the occurrence of phase transformation of RA. In addition, the strain at which significant transformation from RA to martensite occurs in the QPA

samples is higher than that in the QPQ one, which is attributed to the preferential deformation of carbide-free ferrite in the early strain stage. The strains where RA begins to transform to martensite remarkably for both QPQ (0.06) and QPA (0.08) samples are in a good consistence with the onset strains of the second stage in work hardening. The change of volume fraction of RA against indicates the analysis of the two-stage work hardening behavior of the studied steel is reasonable.

The oscillation of the curve in the first stage when the partitioning temperature reaches 450 ℃ (Fig. 7b) is thought to be caused by the generation of Cottrell atmosphere. The work of Zhao et al. [31] indicated that the yield strength of ultra-low carbon steel increased with the increase of aging time, and the strengthening was caused by the interaction of dislocations and the Cottrell atmosphere. Carbon has strong diffusion ability when partitioned at 450 ℃, and it could diffuse sufficiently during the subsequent air-cooling process and concentrates around dislocations to generate the Cottrell atmosphere which has the effect of solution strengthening. Except for the precipitation of carbides, this gives another good explanation for the increase of yield strength with the partitioning temperature increasing from 420 ℃ to 450 ℃ in Fig.5. The effect of this phenomenon on the Q-P steels will be analyzed in future work.

5. Conclusion

In this research, a low carbon Nb-microalloyed Q-P steel was studied in details by tensile test, XRD, SEM and TEM. The main conclusions are summarized as follows:

1) Air-cooling treatment enhanced the elongation, especially when the steel was partitioned at 420℃. The strength of the QPA samples was lower than that of the QPQ ones, while the QPA samples had much higher elongation and better mechanical properties than the QPQ ones.
2) The QPQ samples consisted of martensite and RA. The QPA samples, however, exhibited a multiphase microstructure of carbide-free ferrite, martensite and RA. The volume fraction

of RA in the QPA samples was higher than that in the QPQ ones.

3) The studied steel exhibited a two-stage work hardening behavior. In the first stage, the martensite deformed plastically for the QPQ samples. For the QPA samples, however, the carbide-free ferrite deformed preferentially, and then, the carbide-free ferrite and martensite co-deformed for the QPA ones. The strain at which significant transformation from RA to martensite occured in the QPA samples was higher than that in the QPQ one, which was attributed to the preferential deformation of carbide-free ferrite in the early strain stage. In the second stage, TRIP effect of RA provided a relatively high hardening ability and plateaus of work hardening exponents were observed until fracture for all the samples.

Acknowledgments

The present study was financially supported by the National Natural Science Foundation of China (No: 51031001).

References

[1] European Commission, The Strategic Research Agenda of the European Steel Technology Platform, ESTEP, Belgium; (2005) p. 49.
[2] J. G. Speer, D. V. Edmonds, F. C. Rizzo, et al., Curr. Opin. Solid STM. 8 (2004) 219-237.
[3] J. G. Speer, A. M. Streicher, D. K. Matlock, et al., Minerals Metal and Mater. (2003) 505-522.
[4] J. G. Speer, F. C. Rizzo, D. K. Matlock, et al., Mater. Res. 8 (2005) 417-423.
[5] D. V. Edmondsa, K. Hea, F. C. Rizzo, et al., Mater. Sci. Eng. A 438-440 (2006) 25-34.
[6] F. L. H. Gerdemann, J. G. Speer, D. K. Matlock, Mater. Sci. Technol. 1 (2004) 439-449.
[7] V. F. Zackay, E. R. Parker, D. Fahr, et al., Trans of ASM. 60 (1967) 252.
[8] W. C. Leslie, G. G. Rauch, Metall. Trans. A 9 (1978) 343.
[9] X. D. Wang, B. X. Huang, Y. H. Rong, et al., Mater. Sci. Technol. 22 (2006) 532.
[10] E. Girault, A. Mertens, P. Jacques, et al., Scr. Mater. 44 (2001) 885.
[11] M. J. Santofimia, J. G. Speer, A. J. Clarke, et al., Acta Materialia. 57 (2009) 4548-4557.
[12] A. J. Clarke, J. G. Speer, D. K. Matlock, et al., Scripta Materialia. 61 (2009) 149-152.
[13] H. K. D. H. Bhadeshia, D. V. Edmonds, Met. Trans. A 10 (1979) 895.
[14] M. F. Gallagher, J. G. Speer, D. K. Matlock, et al., Proceedings of the 44th Mechanical Working and Steel Processing Conference, Warrendale, PA: ISS,2002, pp. 153-172.

[15] E. Keehan, L. Karlsson, H. O. Andren, et al., Sci. Technol. Weld. Joi. 11 (2006) 19-24.
[16] Seung Chul Baik, Seongju Kim, Young Sool Jin, et al., ISIJ Int. 41/3 (2001) 290.
[17] A. Z. Hanzaki, P. D. Hodgson, S. Yue, ISIJ Int. 35/1 (1995) 79.
[18] Shunichi Hashimoto, Shushi Ikeda, Koh-ichi Sugimoto, et al., ISIJ Int. 44/9 (2004) 1590.
[19] Z. C. Wang, S. J. Kim, C. G. Lee, et al., J. Mater. Process. Tech. 151 (2004) 141-145.
[20] Z. Li, D. Wu, ISIJ Int. 46/1 (2006) 121-128.
[21] Krauss G, Thompson SW, ISIJ Int. 35 (1995fe) 937.
[22] K. Zhang, M. H. Zhang, Z. H. Guo, et al., Mater. Sci. Eng. A 528 (2011) 8486-8491.
[23] N. Zhong, X. D. Wang, Y. H. Rong, et al., J Mater. Sci. Technol. 22 (2006) 751.
[24] J. H. Hollomon, Trans. AIME 162 (1945) 268-290.
[25] D. P. Koistinen, R. E. Marburger. Acta Metall 7 (1959) 59.
[26] S. Zaefferer, J. Ohlert, W. Bleck, Acta Mater. 52 (2004) 2765-2778.
[27] P. Jacques, E. Girault, T. Catlin, et al., Mater. Sci. Eng. A 475 (1999) 273–275.
[28] R.J. Moat, S.Y. Zhang, J. Kelleher, et al., Acta Mater. 60 (2012) 6931-6939.
[29] J. Lian, Z. Jiang, J. Liu, Mater. Sci. Eng. A 147 (1991) 55-65.
[30] Kohichi Sugimoto, Noboru Usui, Mitsuyuki Kobayashi, et al., ISIJ International, 32 (1992), 1311-1318.
[31] J. Z. Zhao, A. K. De, B. C. De Cooman, Mater. Lett. 44 (2000) 374-378.

Figure and Table Captions

Table 1 Chemical compositions of the experimental steel (wt. %)

Fig. 1. Dilatation vs. temeprature curve of experimental steel. Ac1, Ac3 and Ms are austenitisation starting and finishing temperatures and starting temperature of martensite transformation, respectively.

Fig. 2. Schematic heat cycle used in this study.

Fig. 3. SEM micrographs of the (a, b, c, d) QPA and (e, f, g, h) QPQ samples quenched at 260 ℃ and partitioned at different temperatures: (a, e) 350 ℃, (b, f) 390 ℃, (c, g) 420 ℃ and (d, h) 450 ℃.

Fig. 4. TEM micrographs of RA in the undeformed samples quenched at 260 ℃ and partitioned at 390 ℃ followed by (a, b, c) water quenching and (d, e, f) air-cooling: (a, d) BF images, (b, e) DF images, (c) SAED of RA, and (f) SAED of RA and martensite (N-W relationship).

Fig. 5. Mechanical properties of Q-P steel as a function of partitioning temperature: (a) UTS and YS; (b) TE and PSE.

Fig. 6. RA fraction of samples as a function of partitioning temperature after different cooling styles.

Fig.7. Plots of instantaneous work hardening exponent (n_i) vs. ture strain (ε_t) for studied steel with different cooling styles after partitioning at different temperatures from 350 ℃ to 450 ℃: (a) QPQ samples, (b) QPA samples.

Fig. 8. Variation of the transformed RA volume fraction with strain for the QPQ and QPA samples quenched at 260 ℃ and partitioned at 390 ℃.

Table 1 Chemical compositions of the experimental steel (wt. %)

C	Mn	Si	Al	Nb	P	S
0.19	1.53	1.52	0.14	0.048	0.0071	0.0083

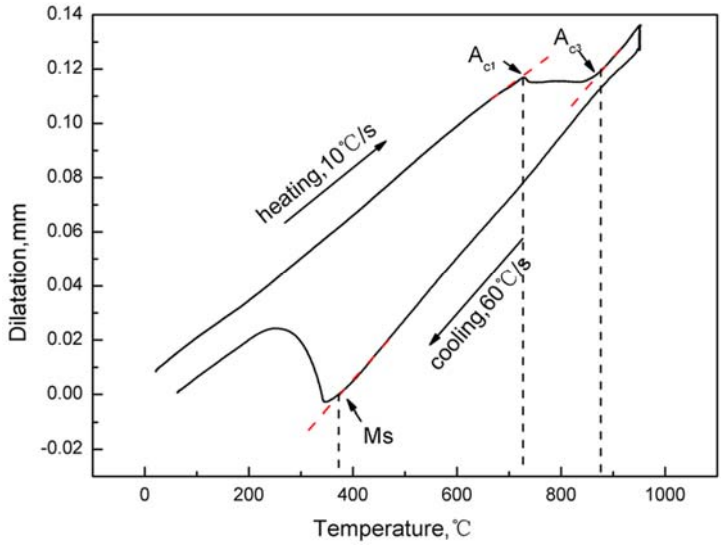

Fig. 1. Dilatation vs. temeprature curve of experimental steel. Ac1, Ac3 and Ms are austenitisation starting and finishing temperatures and starting temperature of martensite transformation, respectively.

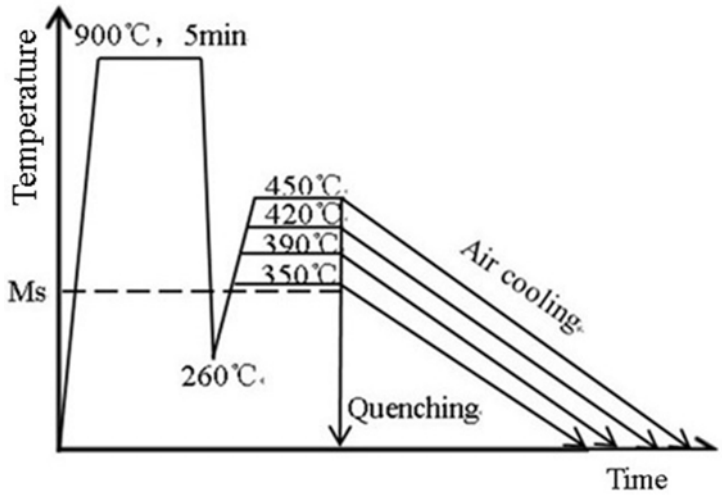

Fig.2. Schematic heat cycle used in this study.

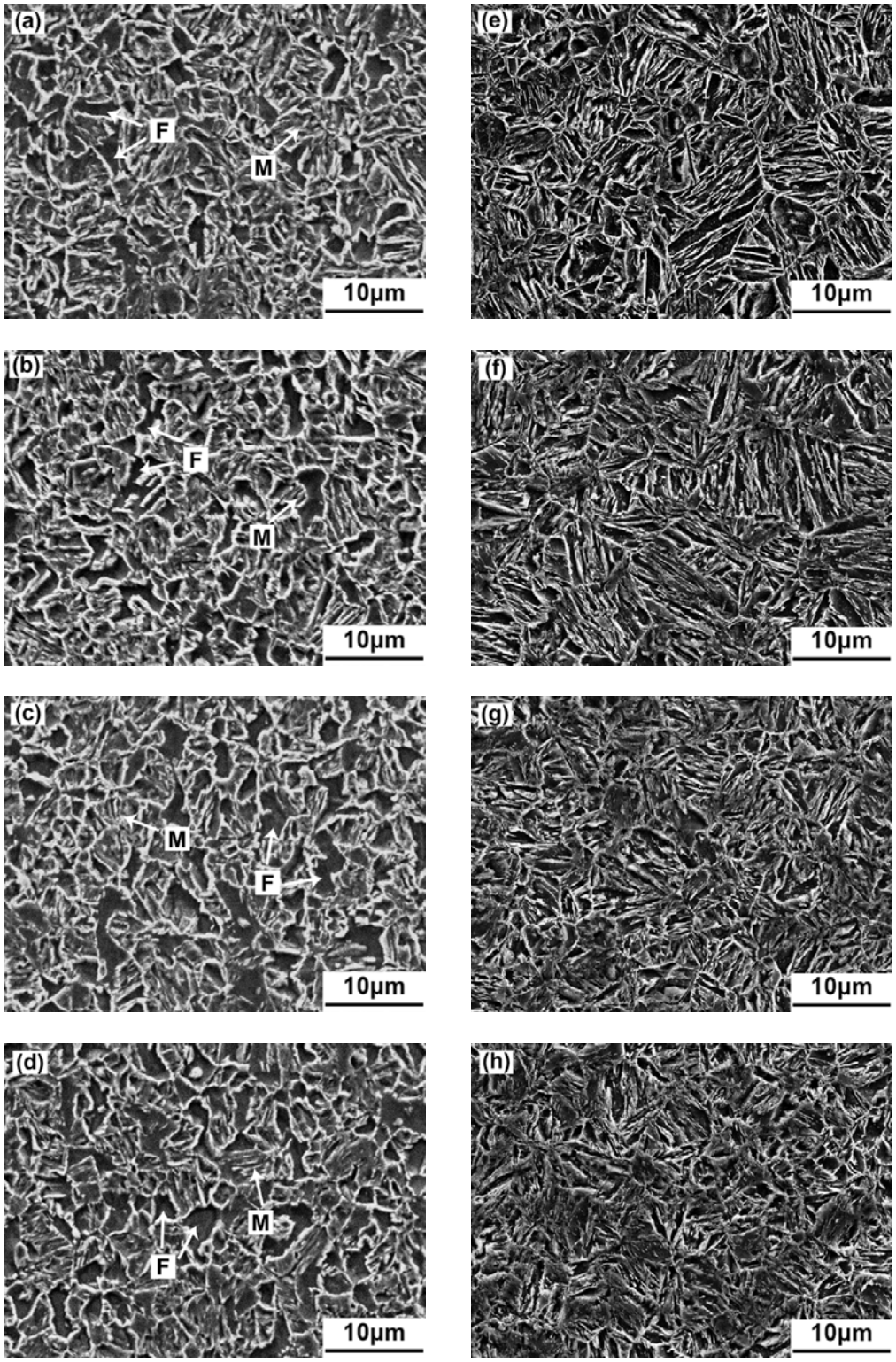

Fig. 3. SEM micrographs of the (a, b, c, d) QPA and (e, f, g, h) QPQ samples quenched at 260 ℃ and partitioned at different temperatures: (a, e) 350 ℃, (b, f) 390 ℃, (c, g) 420 ℃ and (d, h) 450 ℃.

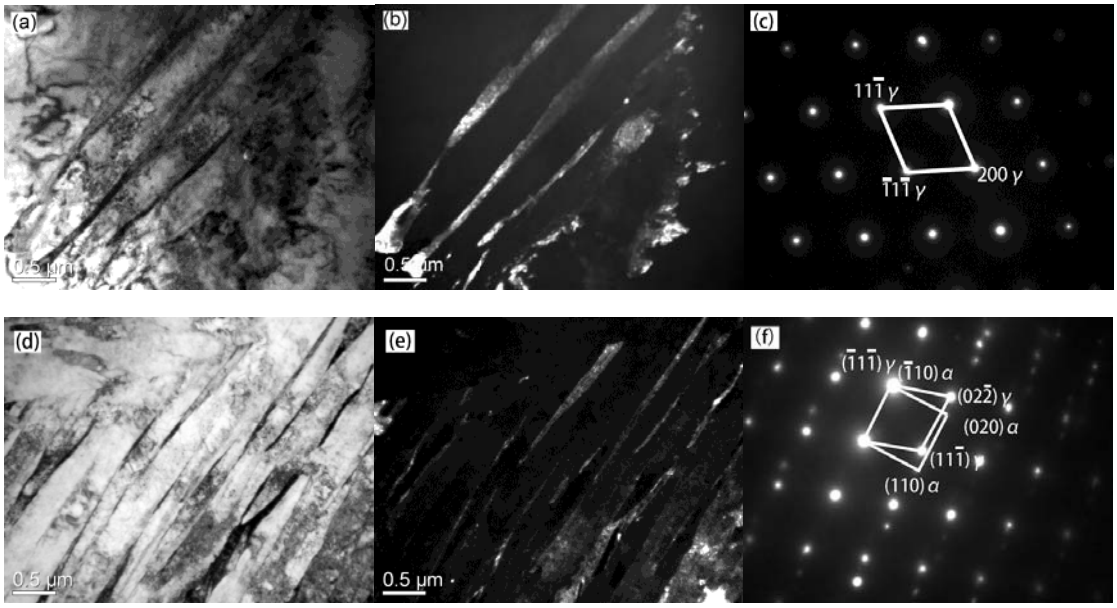

Fig.4. TEM micrographs of RA in the undeformed samples quenched at 260 ℃ and partitioned at 390 ℃ followed by (a, b, c) water quenching and (d, e, f) air-cooling: (a, d) BF images, (b, e) DF images, (c) SAED of RA, and (f) SAED of RA and martensite (N-W relationship).

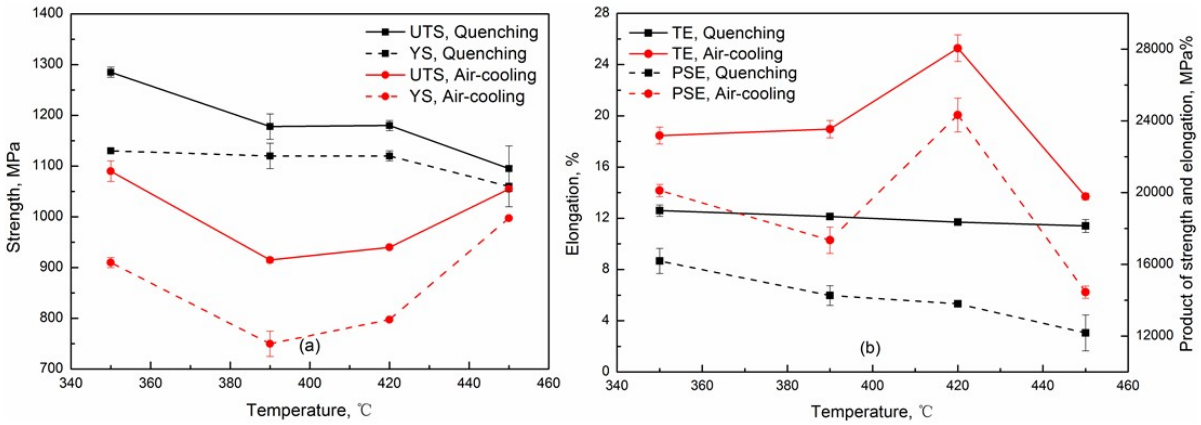

Fig.5. Mechanical properties of Q-P steel as a function of partitioning temperature: (a) UTS and YS; (b) TE and PSE.

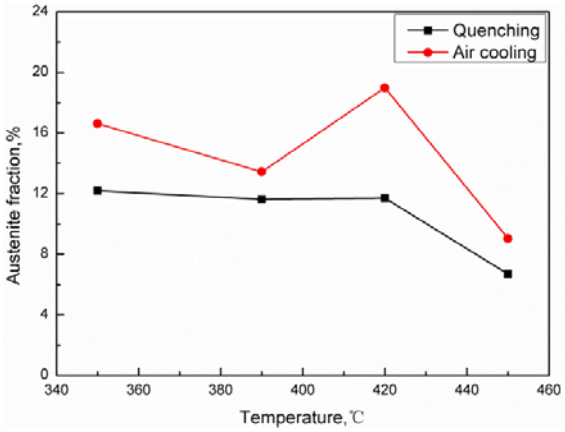

Fig. 6. RA fraction of samples as a function of partitioning temperature after different cooling styles.

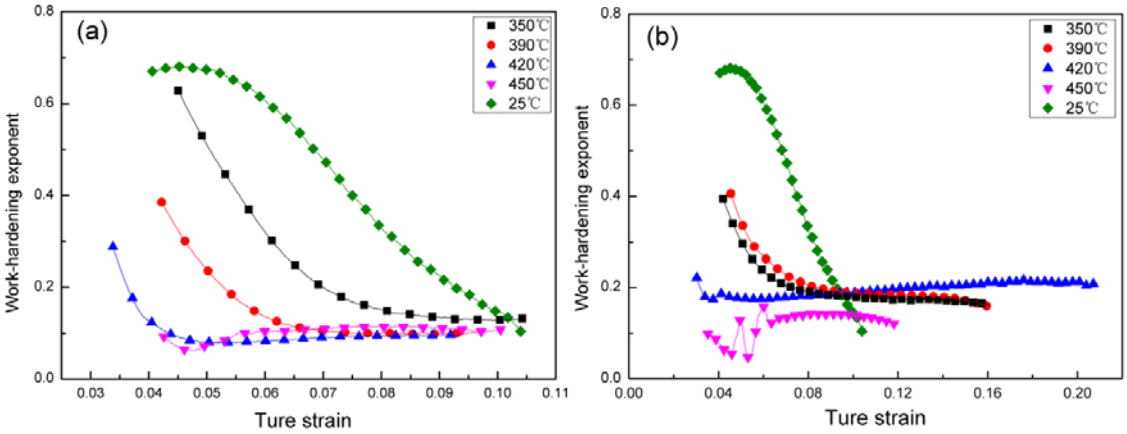

Fig. 7. Plots of instantaneous work hardening exponent (n_i) vs. ture strain (ε_t) for studied steel with different cooling styles after partitioning at different temperatures from 350 ℃ to 450 ℃: (a) QPQ samples, (b) QPA samples.

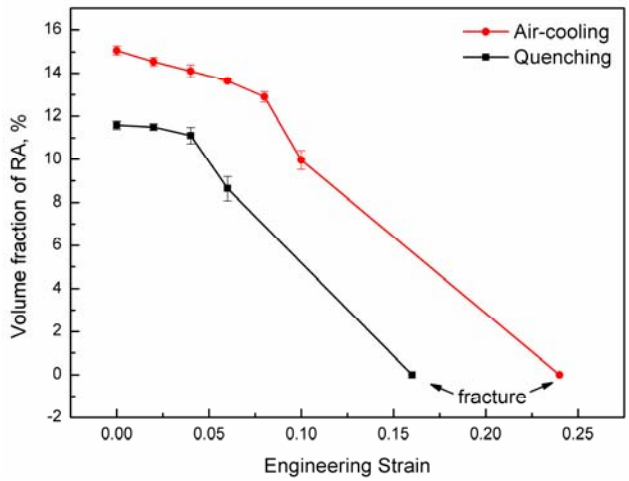

Fig. 8. Variation of the transformed RA volume fraction with strain for the QPQ and QPA samples quenched at 260 ℃ and partitioned at 390 ℃.